

Multibeam optical transmit/receive beamformer using ternary programmable wavelength-division multiplexing technology

Azad Siahmakoun, MEMBER SPIE

Sergio Granieri, MEMBER SPIE

Mark Jaeger

Youzhi Li

Rose-Hulman Institute of Technology
Department of Physics & Optical Engineering
5500 Wabash Avenue
Terre Haute, Indiana 47803
E-mail: azad.siahmakoun@rose-hulman.edu

Abstract. An optical beamformer capable of controlling a phased array antenna in receive/transmit mode for multiple simultaneous independent rf beams is proposed. The processor can be programmed to sweep the antenna aperture following an independent angular sequence for each rf beam. A two-beam two-channel version of the beamformer has been experimentally demonstrated. The optical beamformer processes two rf beams and it is based on a ternary array of three delay lines. Measurements are performed for both receive and transmit modes and for rf signals between 0.5 and 1.5 GHz. We present beam pattern results showing that two independent beams can be steered simultaneously. In the transmit mode both rf beams are characterized for a broadside target position. In the receive mode the beamformer performance is characterized by detecting two rf beams independently. © 2005 Society of Photo-Optical Instrumentation Engineers. [DOI: 10.1117/1.2061407]

Subject terms: beam steering; fiber Bragg gratings; rf photonics; true-time delay.

Paper 040923R received Dec. 27, 2004; revised manuscript received Mar. 25, 2005; accepted for publication Apr. 6, 2005; published online Oct. 4, 2005.

1 Introduction

Many rf and microwave systems, such as high-resolution phased-array antennas and signal processing electronics, require true-time delay (TTD) phase shifters. In such systems, the individual transmit/receive (T/R) element control allows the implementation of beam steering and shaping. In conventional rf systems, TTD is achieved by switching to different lengths of electrical cable. However, these implementations tend to be bulky, heavy, and susceptible to electromagnetic interference. The use of photonics for phased array antennas control is an active field of research, which has helped to overcome some of the problems mentioned above. Fiber-optic systems can provide a lightweight, compact, low-cost phased-array antenna processor, which is immune to electromagnetic interference. Several optical approaches for both phase-based and TTD-type antenna control have been proposed.¹

Photonics systems have been used in applications for providing optical time delays. A possible approach to achieve different time delays is to use a binary delay line configuration in which the fiber-optic optical signal is routed by optical switches through the lines to obtain selected delays.² The use of ternary architectures in optical beamformers and programmable arrays of delay lines is considered in Refs. 3 and 4. To introduce time delays between rf signals, optical beamforming networks can also take advantage of wavelength division multiplexing (WDM) encoding. Radio-frequency signals from/to each T/R element of the antenna are coded using optical carriers with different wavelengths. Thus, different time delays can be introduced between different optical carriers using

wavelength dependent components such as fiber Bragg gratings (FBG) or high-dispersion fiber.⁵⁻⁸ Using this technique, a beamformer capable of process-independent rf beams in receive mode⁹ and receive/transmit modes¹⁰ is demonstrated. In addition, several optical processors using far-field diffraction and acousto-optic modulation to drive a multibeam antenna array have been also proposed.¹¹⁻¹³

Our paper describes an optical beamformer that allows TTD control of multiple simultaneous rf beams using WDM components. The rf signals, which feed the T/R elements of the phased antenna array, are coded using optical carriers with different wavelengths. The beamformer is based on a ternary array of optical delay lines. Delay lines, which are constructed by a sequence of FBG, are interconnected by standard fiber components such as optical switches and circulators. Multiple beam processing is achieved by encoding signals associated with each rf beam by a different WDM optical channel. This allows the beamformer to receive and transmit each beam independently with a wide variety of programmable time delays. The present system is able to provide 15 time-delay configurations with an equivalent resolution of 4 bits in a binary beamformer.

In Sec. 2 we describe a two-beam two-channel optical beamformer in transmit and receive modes. The beamformer characterization is discussed in Sec. 3. Concluding remarks are given in Sec. 4.

2 System Overview

The beamformer in transmit mode is shown schematically in Fig. 1(a). Four laser diodes are utilized to provide optical carriers with wavelengths from λ_1 to λ_4 for four different WDM channels. Each pair of wavelengths, odd-numbered and even-numbered channels, carries information of one rf

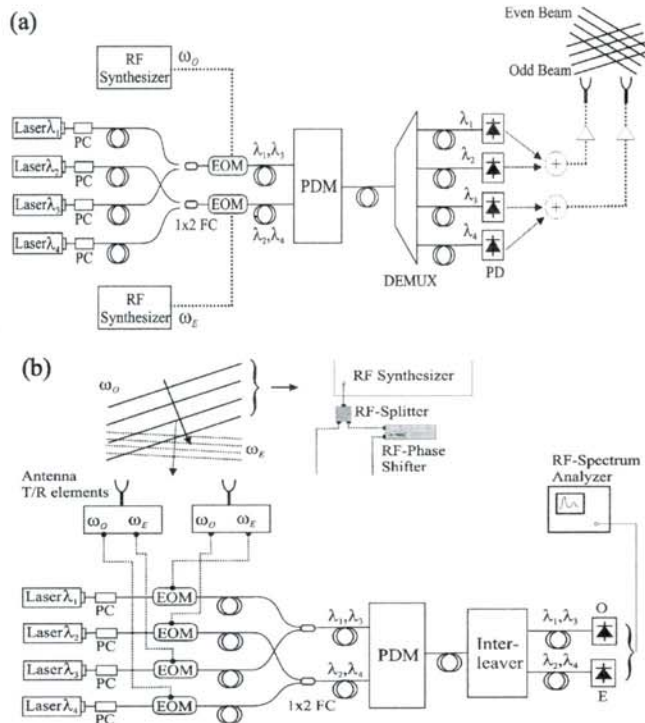


Fig. 1 Two-beam two-channel optical beamformer: (a) transmit mode configuration; (b) receive mode configuration. PC: polarization controller, EOM: electro-optic modulator, FC: fiber coupler, PD: photodetector.

beam independently. In this approach one rf beam is controlled by the odd channels (λ_1 and λ_3) while the second beam is processed via the even channels (λ_2 and λ_4). Odd and even channels are coupled using two 2×1 fiber couplers. The combined odd and even channels are separately modulated with rf signals using two Mach-Zender electro-optic modulators (EOM). Modulation of multiplexed channels ensures zero phase delay between the rf signals before the optical carriers are processed. The modulated optical carriers feed the programmable dispersion matrix (PDM), which performs the TTD processing. The PDM is capable of providing independent time delays for the even and odd channels. For each configuration of the PDM, λ_2 lags λ_4 and λ_1 lags λ_3 by independent time periods $\Delta\tau_O$ and $\Delta\tau_E$ for odd channels and even channels, respectively. At the output of the PDM, after the proper phase difference is set, optical signals are demultiplexed. Four broadband photodetectors, in a direct detection configuration, recover the processed rf signals. Then the rf signals are linearly combined and amplified before feeding the antenna T/R elements.

A schematic of the two-beam optical beamformer in receive mode is shown in Fig. 1(b). Incoming rf beams from two targets with different frequencies ω_O and ω_E are received by two antenna array elements. Radio-frequency bandpass filters split the signal at each antenna element according to their frequency. Even and odd optical channels are modulated by the signals RF_E and RF_O , respectively. The phase difference between the antenna elements for each rf beam $\Delta\phi$ depends on the target angular position ϕ as $\phi = \arcsin(\Delta\phi c / \omega\Lambda)$, where c is the speed of light, Λ is the separation of the antenna T/R elements, and ω is the

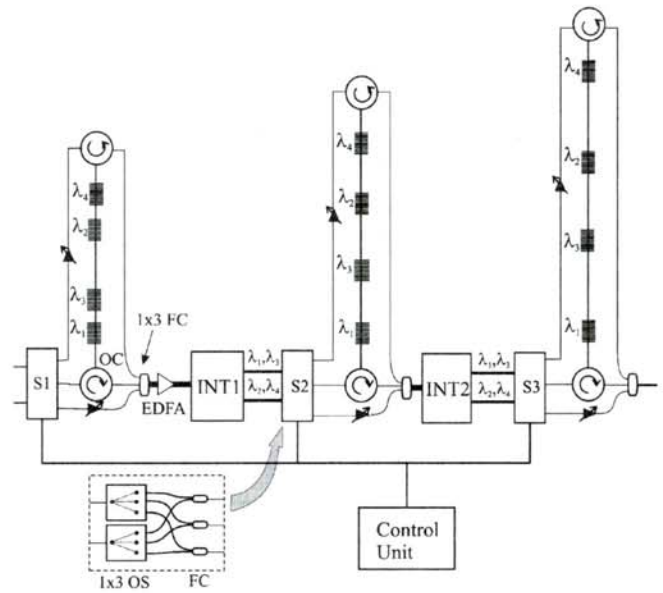


Fig. 2 Schematic of the ternary PDM. The PDM can be set to provide 15 different delay configurations. This performance is similar to a 3-bit binary PDM. S: optical switch, OC: optical circulator, FC: fiber coupler, INT: optical interleaver, EDFA: erbium-doped fiber amplifier.

center frequency of the rf signal. The time delay between the even and odd multiplexed optical channels is corrected independently by the PDM and detected with a single photodetector. The output power of each photodetector is a function of the corrected phase difference between the rf signals for each beam

$$P(\text{dB}) = 10 \log(C_1 + C_2 \cos \Delta\phi), \quad (1)$$

where here $\Delta\phi$ are the phase differences of each rf signal after the PDM, and C_1 and C_2 are proportionality constants that depend on the power of the optical carriers. Thus, the output power in each photodetector is related to each target angular position via this phase difference. When the PDM properly corrects for the phase difference at the antenna elements, a maximum power will be detected for the given target position.

A two-beam two-channel version of the ternary PDM is shown in Fig. 2. This ternary PDM consist of three delay lines for controlling an antenna array with two T/R elements. It can produce 15 different delay configurations for each beam, thus it is capable of pointing the even and odd rf beams independently in 15 different angular directions. In general, the $2^N - 1$ delay configuration version of the ternary PDM consists of an array of $N - 1$ delay lines. Each delay line has four gratings organized into two pairs, where the center wavelength of each FBG matches one of the multiplexed optical channels. The separation between FBG with center wavelengths corresponding to either channel (odd or even) is increased in multiples of two from delay line to delay line. Thus, time delays between channels are proportional to these FBG separations. The separation of two adjacent gratings corresponding to either channels (odd or even) of the i 'th line are given by $\Delta L_i = 2^{i-1} \Delta L_1$, where ΔL_1 is the minimum separation between the Bragg gratings of line 1 that may be different for odd and even channels.

The time delay provided by the i 'th line for either odd or even channels is $\tau_i = (2n_{\text{eff}}\Delta L_i)/c$, where n_{eff} is the effective refractive index of the fiber. The programmable optical switches configure independent propagation of the even and odd channels throughout the PDM. Each switch unit consists of two 1×3 optical switches and three 1×2 couplers. The upper switch in the subset shown in Fig. 2 directs the odd channels either to the top or to the bottom end of the delay line, for introducing a time delay between the channels or to bypass the delay line. Meanwhile the lower switch performs a similar function as described above for the even channels. The 1×2 couplers are used to combine the outputs from both switches; those either going to delay or bypass lines. Circulators route the optical channels to/from both ends of the delay lines. A 1×3 coupler is used to combine the optical signals coming from the delay line and the bypass line for a second time. After the 1×3 coupler, an interleaver is used to separate the four multiplexed channels again into odd and even channels. Each interleaver is followed by a switch unit that is connected to the next delay line. This structure repeats itself until the 1×3 coupler after the last delay line. With this configuration both positive and negative time delays are possible. This means λ_2 lags λ_4 by τ_i when the signal is routed to the bottom end of the i 'th delay line and λ_2 leads λ_4 by the same period when the signal is routed to its top end. Therefore, both rf beams generated by these time delays can be steered in both positive and negative angular directions relative to the broadside. Each possible time delay introduced by the PDM on each rf beam can be calculated from

$$\tau(m) = \sum_{i=1}^{N-1} a_{i,m} \tau_i, \quad (2)$$

where the value of the constant $a_{i,m}$ depends on the optical signal path and m is an index representing each switch configuration. The optical signal can be routed to the bottom end or top end of the i 'th delay line being $a_{i,m} = 1$ and $a_{i,m} = -1$ respectively. On the other hand, when light is bypassing the i 'th delay line $a_{i,m} = 0$. Time delays, which are integer multiples of the minimum delay τ_1 , range from $-(2^{N-1})\tau_1$ to $+(2^{N-1})\tau_1$. This results in a symmetrical distribution around zero delay (broadside) with similar resolution to a N -bit binary PDM.³ The achievable steering angles ϕ_m for either even or odd rf beams are

$$\phi_m = \arcsin\left(\frac{cm\tau_1}{\Lambda}\right) \quad m = 0, 1, \dots, 7 \quad (3)$$

where Λ is the separation between antenna array T/R elements. Since the switch configuration m can be set independently for each beam, the steering angles are therefore independent. The minimum time delay associated with the first delay line is directly related to the resolution of the beamformer. The minimum resolvable angle for both beams can be calculated by setting $m=1$ in Eq. (3). However, in order to improve the angular resolution of the system a shorter minimum time delay is required, i.e., the minimum grating separation must be decreased.

3 Results

The center wavelengths of the four gratings in each line match the International Telecommunications Union (ITU) frequency channels 30 through 33 with a maximum deviation of ± 0.1 nm. All the gratings have reflectivity around 98% and FWHM between 0.4 and 0.6 nm. The separation between the FBG associated with the even channels are 14 ± 2 mm, 28 ± 2 mm, and 58 ± 2 mm for lines 1 through 3, respectively. For the FBG of odd optical channels the separations are 15 ± 2 mm, 30 ± 2 mm, and 60 ± 2 mm. Based on these separations, the minimum time delay is calculated to be 137.11 ps for the even channels and 146.90 ps for the odd channels. In order to measure the minimum time delays, a vector network analyzer is used as a source to drive the electro-optic modulators and to detect the rf signal from a photodiode. By direct measurement of the S_{12} parameter the time delay introduced by the system can be obtained as in Ref. 10. The measured minimum time delays for the odd and even channels are 135.87 ps and 132.24 ps, respectively. Variations from the calculated values can be attributed to grating spacing errors. A data acquisition unit that is interfaced with a computer controls the six programmable optical switches. Based on the electronic control and switching time, the reconfiguration time for the PDM is 5 ms. If the beamformer steers the main lobe across a far-field observer located at broadside, the measured rf power levels of the transmitted beams P at the observer are given by Eq. (1). If isotropic radiating elements are assumed the transmitted power depends on the time delays introduced by the PDM between the optical carriers through phase differences $\Delta\varphi$ and the power of the optical carriers at the output of the system through constants C_1 and C_2 . Since a uniform excitation of the array elements is assumed then the optical powers have to be independent of the switching configuration m of the PDM. A similar argument can be given for the transmit mode. However, in practice, the optical loss throughout the PDM for each switch configuration is different. In order to achieve optical output powers that are independent of the switch configuration, optical attenuators are added to the PDM. If a delay line is bypassed, the optical carrier neither passes through the circulator nor is reflected by the FBG. Therefore, the insertion loss is quite different depending on whether the delay line is or is not in the path of the optical carrier. In addition, variations in the optical output power can also arise from different reflectivity of the FBG as well as wavelength-dependent insertion loss in the multiplexer. To provide equal loss levels, optical attenuators are placed in two of the three possible paths of each delay line. The attenuation level is set to compensate for the insertion loss of the circulators and the reflection loss of the FBG. To compensate the optical loss, an erbium-doped fiber amplifier (EDFA) with 26-dB gain is added in the system as shown in Fig. 2.

In transmit-mode measurements, even and odd carriers are modulated by a 10-GHz-bandwidth LiNbO₃ EOM of $V_\pi = 4.5$ V with rf signals provided by two signal generators. The detection scheme in Fig. 1(a) is slightly modified just for measurement purposes. The four carriers coupled at the output of the PDM are detected by a single photodetector. As the rf signals related to the even and odd channels have different frequencies, the rf power out of the photode-

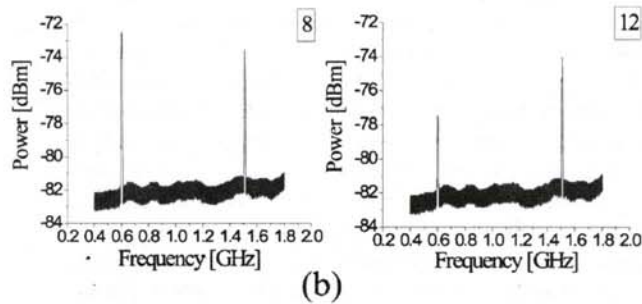
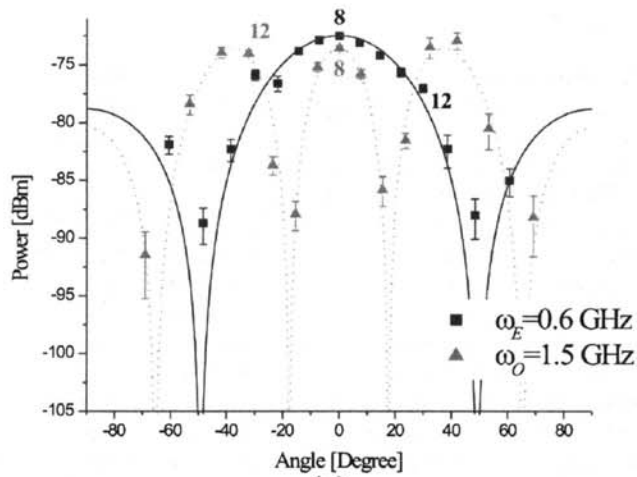


Fig. 3 (a) Simultaneous transmission beampatterns for an even rf beam at 0.6 GHz and an odd rf beam at 1.5 GHz. (b) Selected spectral power profiles. Each profile is related to a particular switch configuration of the PDM and its number is shown in the beampattern (a). Profile 8 corresponds to the switch configuration $m_{\text{Odd}}=0$, $m_{\text{Even}}=0$ and profile 12 to $m_{\text{Odd}}=-4$, $m_{\text{Even}}=4$.

tector for each beam is detected using an rf spectrum analyzer. Notice that rf signals in both even and odd channels are in phase at the input of the PDM. The rf phase shift introduced by the PDM is transformed in power variations according to Eq. (1). These power variations represent the power of a single received by an observer at broadside (or 0-deg azimuth angular position) for different switch configurations of the PDM. Consequently, beampatterns are characterized for an observer at the broadside position when the main lobe of the transmit beam is steered at different angles. The steering angle that corresponds to a given delay configuration can be calculated from Eq. (3). Simultaneous transmission beampatterns for the odd rf beam at 1.5 GHz and the even rf beam at 0.6 GHz together with the theoretical curves (even beam: solid line, odd beam: dotted line) are presented in Fig. 3(a). To illustrate that both beams are simultaneously controlled by the beamformer, two selected spectral power profiles of the two detected rf center frequencies are shown below the beampatterns in Fig. 3(b). To demonstrate that the two beams can be independently steered, the odd beam is steered from switching position $m_{\text{Odd}}=7$ through -7 (which correspond to azimuth angles from 69 to -69 deg), while the even beam is steered from switching position $m_{\text{Even}}=-7$ to 7 (corresponding to azimuth angles of -61 to 61 deg). To illustrate the performance of the beamformer for two close rf

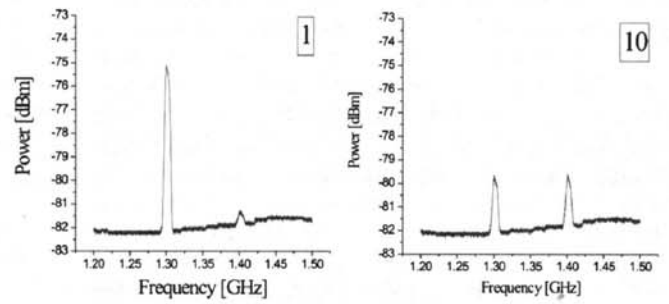
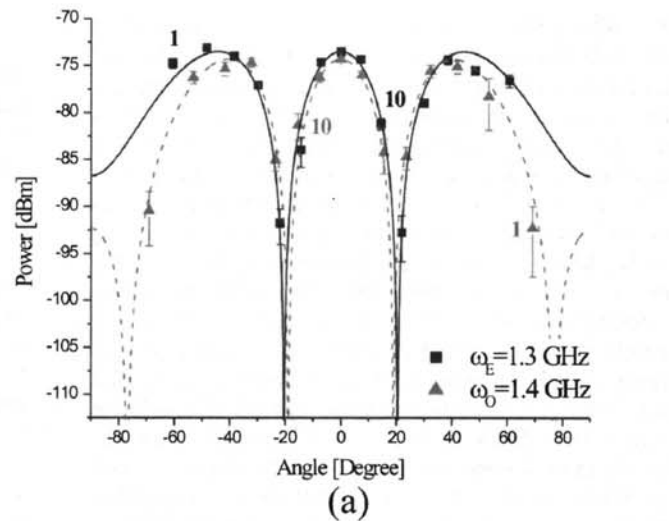


Fig. 4 (a) Simultaneous Transmission beampatterns for an even rf beam at 1.3 GHz and an odd RF beam at 1.4 GHz. (b) Selected spectral power profiles. Each profile is related to a particular switch configuration of the PDM and its number is shown in the beampattern (a). Profile 1 corresponds to the switch configuration $m_{\text{Odd}}=-7$, $m_{\text{Even}}=7$ and profile 10 to $m_{\text{Odd}}=-2$, $m_{\text{Even}}=2$.

center frequencies, Fig. 4 shows the beampattern results for the even rf beam at 1.3 GHz and the odd rf beam at 1.4 GHz. Even though data points show good agreement with the theoretical curves, the odd rf beam exhibits a larger deviation of power levels in beampattern measurements. It was determined that these deviations are attributed to cross-talk noise of FBGs associated with odd channels.

Measurements in receive-mode configuration are performed for two rf beams simultaneously by characterizing the array factor of the antenna for rf signals of different frequencies. The array factor is equivalent to the beampattern when isotropic antenna T/R elements are considered. In this characterization, the PDM is fixed to one switching position and the output power of the system is measured while a simulated target moves past the antenna elements. The experimental setup used for receive measurements is a modified version of the system shown in Fig. 1(b). The performance of the PDM is tested for each rf beam independently. Cross-talk results of WDM channels in the system lead us to conclude that the two beampatterns can be measured separately with no significant difference in the performance of the beamformer. An rf signal generator simulates an incoming rf beam from a target. The output of

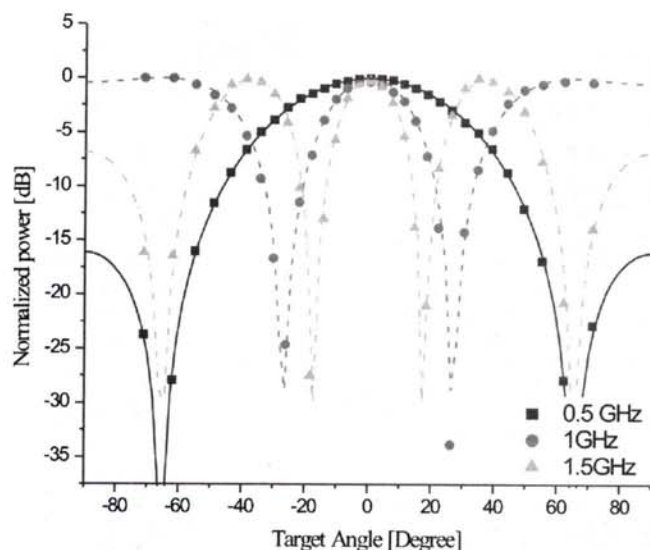


Fig. 5 Beam patterns measured in receive mode for the odd channels at rf signals of 0.5, 1, and 1.5 GHz. The switch configuration of the PDM is $m=0$ and the main lobe is located at broadside.

the signal generator is split and sent to two EOMs. An rf attenuator is used to compensate any difference in the modulation performance of the two EOM. To simulate the phase difference between antenna elements due to the moving target, an rf phase shifter is introduced before one of the modulators. For each selected rf center frequency, the output signal from the photodiode is measured for 31 discrete phase-shifter settings using an rf spectrum analyzer. The phase-shift sequence ranges from 0 deg/GHz to 900 deg/GHz. The angular direction or azimuth ϕ of the target is related to the phase difference $\Delta\phi$ introduced by the phase shifter by $\phi = \arcsin((c\Delta\phi)/(\omega_{RF}\Lambda))$. The antenna element spacing Λ is assumed to be $0.5\lambda_{RF}$ at 460 MHz, which enables the beamformer to process signals with azimuth angles up to 69 deg and 61 deg for odd and even beams, respectively. Beam patterns are measured and analyzed for the even and odd beams for all possible switch configurations. Figure 5(a) shows the measured even and odd beam patterns along with fitted curves for three rf signals at 0.5, 1, and 1.5 GHz when the PDM is configured for $m=0$. At this particular switch position, the optical carriers do not pass through any of the delay lines of the PDM. For this reason, a maximum in the output power is detected when the simulated target is at the broadside position.

4 Conclusion

We have proposed a multibeam WDM optical beamformer capable of driving a phased array antenna in receive and transmit modes. The concept is demonstrated by a simple two-beam two-channel version of the processor. The system is based on an array of three delay lines, which provide the antenna an equivalent angular resolution of 4 bits. That is, two beams can be pointed independently in 15 different angular directions. In this prototype the possible angular range of the antenna is -61 to $+61$ deg and -69 to $+69$ deg for two independent rf beams.

These experiments demonstrate a working prototype of the proposed T/R beamformer for the rf frequency range of

0.5 to 1.5 GHz. The transmit mode is characterized for a broadside target across which the two rf beams are steered. In the receive mode the beamformer is characterized by detecting two rf beams from separate targets. Results for both transmit and receive measurements show good agreement with the theoretical model.

No additional optical components such as circulators, switches, or attenuators will be necessary to scale up this proposed PDM for phased-array antennas with a large number of T/R elements. This upgrade only requires an increase in the number of FBGs in each delay line. However, in order to scale up the system for a higher number of rf beams, multipoint interleavers and more optical switches are needed. The number of WDM channels needed is proportional to the number of rf beams and antenna T/R elements. Therefore a laser source with wide bandwidth and broadband optical components suitable for that wavelength range are required for multibeam processing. The ternary PDM requires one less delay line of FBGs in order to obtain similar performance as its binary counterpart.¹⁰ This advantage is critical when a large number of FBGs have to be fabricated in a single delay line.

Temperature changes do not introduce significant performance degradation in our controlled laboratory environment since the sensitivity of the Bragg wavelength with the temperature is about 10 pm/°C. However, a PDM prototype designed to work in a harsh environment requires thermally insulated FBGs.

Acknowledgments

The authors would like to thank Dr. Daniel S. Purdy of the Office of Naval Research for his support of this project under the contract number N00014-00-0782.

References

1. N. Riza, Ed., *Selected Papers on Photonic Control Systems for Phased Array Antennas*, SPIE Milestone Series Vol. MS 136, SPIE Press, Bellingham (1997).
2. A. P. Goutzoulis, D. K. Davies, and J. M. Zomp, "Prototype binary fiber optic delay line," *Opt. Eng.* **28**, 1193–1202 (1989).
3. S. Palit, M. Jaeger, S. Granieri, B. Black, J. Chestnut, and A. Siahmakoun, "5-bit programmable binary and ternary architectures for an optical transmit/receive beamformer," *IEICE Trans. Electron.* **E86-C**, 1203–1208 (2003).
4. N. A. Riza and N. Madamopoulos, "Phased array antenna maximum compression reversible photonic beamformer," *Appl. Opt.* **36**, 983–996 (1997).
5. R. Soref, "Fiber grating prism for true time delay beamsteering," *Fiber Integr. Opt.* **15**, 325–333 (1996).
6. H. Zmuda, A. Soref, P. Payson, S. Johns, and E. Toughlian, "Photonic beamformer for phased array antennas using a fiber grating prism," *IEEE Photonics Technol. Lett.* **9**, 241–243 (1997).
7. D. Tong and M. Wu, "Transmit/receive module of multiwavelength optically controlled phased-array antennas," *IEEE Photonics Technol. Lett.* **10**, 1018–1020 (1998).
8. Y. Liu, J. Yang, and J. Yao, "Continuous true-time-delay beamforming for phased array antenna using a tunable chirped fiber grating delay line," *IEEE Photonics Technol. Lett.* **14**, 1172–1174 (2002).
9. P. J. Matthews, M. Y. Frankel, and R. D. Esman, "A wide-band fiber-optic true-time-steered array receiver capable of multiple independent simultaneous beams," *IEEE Photonics Technol. Lett.* **10**, 722–724 (1998).

10. S. Granieri, M. Jaeger, and A. Siahmakoun, "Multiple beam fiber-optic beamformer with binary array of delay lines," *J. Lightwave Technol.* **21**, 3262–3272 (2003).
11. Y. Ji, K. Inagaki, R. Miura, and Y. Karasawa, "Optical processor for multibeam microwave receive array antennas," *Electron. Lett.* **32**, 822–824 (1996).
12. O. Shibata, K. Inagaki, Y. Karasawa, and Y. Mizuguchi, "Spatial optical beamforming network for receiving-mode multibeam array antenna: proposal and experiment," *IEEE Trans. Microwave Theory Tech.* **50**, 1425–1430 (2002).
13. N. Riza, "An acousto-optic phased-array antenna beamformer for multiple simultaneous beam generation," *IEEE Photonics Technol. Lett.* **4**, 807–809 (1992).



Azad Siahmakoun received BS, and MS, and PhD degrees in physics. He completed his doctoral degree at the University of Arkansas in 1987. He joined the Department of Physics and Applied Optics of Rose-Hulman Institute of Technology in September of 1987 where he is now a professor of physics and optical engineering and the director of Center for Applied Optics Studies. Dr. Siahmakoun has been active in optics education and research. He has recently

developed a microfabrication and MEMS laboratory for teaching undergraduate students. He is the principal investigator of the wide-band optical beamformer and optical delta-sigma modulator that are supported by ONR 2000-2005. His research interests are in the area of optical MEMS, rf photonics, optical analog-to-digital conversion, and optical information processing.



Sergio Granieri received the BS and PhD degrees in physics from University of La Plata, Argentina, in 1993 and 1998, respectively. His doctoral research was concerned with the study and optical generation of the fractional Fourier transform and applications to signal processing. From 1994 to 1998, he worked at Optical Research Center (CIOP), La Plata, Argentina, where he engaged in research on optical information processing. From 1998 to 2000, he was assigned to the Optical Communication Laboratory (LAMECO) at the same institution, to pursue research on erbium-doped fiber amplifiers. Since 2000, he has been principally involved with research on optical control of phased-array antennas for radar applications and optical analog/digital conversion at Center for Applied Optics Studies of Rose-Hulman Institute of Technology, where he has been a visiting assistant professor of physics and optical engineering since 2003.



Mark Jaeger received his BS degree in electrical engineering from the University of Stuttgart, Germany, in 2000, and his MS degree in applied optics from the Rose-Hulman Institute of Technology in 2002. His research interests are in the area of rf photonics, optical analog-to-digital conversion, and optical communication systems. He is presently an electrical engineering PhD candidate at the University of Stuttgart.

Youzhi Li Biography and photograph not available.